Journal of Biological and Environmental Sciences

e-ISSN 1308-2019
https://dergipark.org.tr/en/pub/jbes
http://www.uludag.edu.tr/jbes

2026, 58, 18469002

Received: 20 November 2025
Accepted: 03 February 2026

RESEARCH ARTICLE
https://doi.org/10.5281/zenodo.18469002

Sustainable Copper Removal with Seafood Shells: Biosorption Kinetics and ANN Analysis[A]

Sevda Esma DARAMA[1]* Semra ÇORUH[2]

Abstract: Heavy metal contamination necessitates cost-effective and eco-friendly treatment methods. This study explores the potential of waste seafood shells as a sustainable biosorbent for copper (Cu^{2+}) removal. Batch experiments examined the effects of particle size, contact time, and adsorbent dosage on biosorption. Results confirmed that smaller particle sizes significantly enhanced removal efficiency (>90%) due to increased surface area. While the maximum copper removal was achieved at 40 g L^{-1}, 20 g L^{-1} was identified as the optimum dosage considering both removal efficiency (>90%) and economic feasibility. Adsorption data fitted the Freundlich isotherm and pseudo-second-order kinetic models, indicating multilayer chemisorption on heterogeneous surfaces. Furthermore, a Nonlinear Autoregressive with Exogenous Inputs (NARX) artificial neural network (ANN) was developed. This model accurately predicted copper removal efficiency with a low mean squared error. Findings demonstrate that seafood shells are promising biosorbents, and the integration of ANN modeling offers a powerful tool for optimizing sustainable wastewater treatment systems.

Keywords: Adsorption, ANN, Copper Removal, Isotherms, Kinetics, Seafood Shell

[A] The study does not require approval from an ethics committee. The article has been prepared according to research and publication ethics.

***Corresponding Author:** [1] Sevda Esma DARAMA, Ondokuz Mayıs University, Institute of Graduate Studies, Samsun, Türkiye. sevda.akkaya@uludag.edu.tr, ORCID: 0000-0002-6747-4679
[2] Semre ÇORUH, Ondokuz Mayıs University, Faculty of Engineering, Department of Environmental Engineering, Samsun, Türkiye, semrahcoruh@omu.edu.tr, ORCID: 0000-0002-8306-1890

Atıf/Citation: Darama, S. E, and Çoruh, S. 2026. Sustainable copper removal with seafood shells: Biosorption kinetics and ANN analysis. *Journal of Biological and Environmental Sciences*, 58, 18469002.

Introduction

Wastewater discharges from various industrial activities often contain toxic heavy metals such as chromium, mercury, cadmium, lead, and copper substances known for their persistence, non-biodegradability, and severe ecological risks (Bashir et al., 2020). These contaminants must be effectively removed prior to wastewater reuse or environmental discharge. Unlike organic pollutants, heavy metals do not decompose into harmless by-products (Fiyadh et al., 2023).

Conventional metal removal techniques such as coagulation-precipitation, ion exchange, reverse osmosis, electrodialysis, and solvent extraction are often costly. In contrast, adsorption using low-cost, readily available biosorbents has gained attention for its economic and operational feasibility. Recent studies have focused on biodegradable and accessible materials, including bone and shell wastes, due to their favorable adsorptive properties and environmental sustainability (Bashir et al., 2020; Dutta et al., 2024). Compared to activated carbon and other conventional sorbents, seafood shells are especially attractive due to their abundance and low cost (El Haddad et al., 2014; Monteiro et al., 2016). Copper is of particular concern due to its widespread industrial use and potential toxicity. Although essential in trace amounts for biological functions, excess copper accumulation can lead to severe health issues, including gastrointestinal distress, osteoporosis, and even fatal outcomes (Kusmierek et al., 2025). Primary industrial sources include pickling and electroplating operations (Bashir et al., 2020).

While commercial activated carbon (AC) is a standard benchmark for heavy metal removal due to its high surface area, its regeneration costs remain a barrier. In contrast, waste seafood shells, primarily composed of calcite ($CaCO_3$), offer a low-cost and sustainable alternative that achieves comparable removal efficiencies (>90%) for copper without intensive chemical processing.

Artificial Neural Networks (ANNs) have been effectively used for simulating complex, nonlinear processes in separation science. These computational models emulate human learning and decision-making, offering advantages in processing noisy, incomplete, or nonlinear datasets (Alshahrani et al., 2024). ANNs have been successfully applied to model adsorption phenomena across various studies. Notably, NARX-type recurrent networks, with their superior convergence and generalization capabilities, provide robust frameworks for time-dependent adsorption modeling (Dharmendra, 2024).

This study focuses on copper ion removal via biosorption using waste seafood shells. It investigates the effects of operational parameters on removal efficiency, fits the data to classical isotherm models, and applies a NARX ANN model to predict system performance.

Materials and Methods

Biosorbent Preparation and Characterization

Seafood shells used as biosorbents were collected from a local restaurant in Samsun, Turkey. The shells were thoroughly washed with distilled water to remove residual organic matter and surface contaminants. Cleaned samples were then oven-dried at 70°C for 12 hours. After drying, the shells were crushed and sieved to obtain particles within the 0.063-1 mm size range. These powdered samples were subjected to a secondary drying step at 70°C for 24 hours and subsequently stored in a desiccator to prevent moisture absorption.

To characterize the physicochemical structure and surface morphology of the biosorbent materials, XRD and SEM analyses were carried out. These techniques were employed to identify the crystalline phases and to observe surface textural features, respectively, following the biosorption process. X-ray diffraction (XRD) analysis was performed using a Bruker D8 Advance diffractometer equipped with Cu-Kα radiation (λ = 1.5406 Å) operating at 40 kV and 40 mA. The diffraction patterns were recorded in the 2θ range of 10° to 80° at a scanning rate of 2° min^{-1} with a step size of 0.02°. The XRD measurements were conducted at room temperature under ambient atmospheric conditions. The surface morphology of the biosorbent was examined using a ZEISS EVO LS10 scanning electron microscope. Prior to imaging, the samples were sputter-coated with a thin layer of gold to enhance electrical conductivity. SEM images were captured at various magnifications under an accelerating voltage of 10–15 kV. The analysis was conducted in high-vacuum mode.

Adsorption Experiments

Copper ion (Cu^{2+}) solutions were prepared by dissolving analytical-grade $CuCl_2 \cdot 6H_2O$ in deionized water. Working solutions with initial concentrations of 10, 20, 30, 40, and 50 mg L^{-1} were obtained through serial dilution of the stock solution. The initial pH of the Cu^{2+} solutions was measured as 7.24, and no further pH adjustment was made to simulate natural wastewater conditions.

Batch adsorption experiments were carried out to investigate the effects of various operational parameters, including particle size, adsorbent dosage, initial copper concentration, and contact time. Seafood shell powders of five different particle size ranges (−1 +0.5, −0.5 +0.25, −0.25 +0.125, −0.125 +0.063, and −0.063 +0.0315 mm) were used. Adsorbent dosages were adjusted to 5, 10, 20, 30, and 40 g L^{-1}, and experiments were conducted using 50 mL of Cu^{2+} solution placed in 250 mL erlenmeyer flasks. The mixtures were agitated at 150 rpm and 25 °C for 60 min. using an orbital shaker. To evaluate kinetic behavior, contact times of 1, 5, 15, 30, 60, 120, and 240 minutes were tested.

All adsorption experiments were conducted in triplicate to ensure reproducibility. Data points reported in the figures represent the mean values, and error bars indicate the standard deviations.

At the end of the predetermined contact time, the solutions were filtered using 0.45 μm syringe membrane filters. Copper concentrations in the filtrates were analyzed using atomic absorption spectroscopy (AAS, Unicam-929) equipped with a copper-specific hollow cathode lamp.

At the end of the predetermined contact time, the solutions were filtered using 0.45 μm syringe membrane filters. Copper concentrations in the filtrates were analyzed using atomic absorption spectroscopy (AAS, Unicam-929) equipped with a copper-specific hollow cathode lamp.

The copper removal efficiency (%) was calculated using the following Equation (1):

$$R = \frac{C_0 - C_e}{C_0}\ x\ 100 \quad (1)$$

where Co is the initial concentration of Cu^{2+} (mg L^{-1}), Ce is the equilibrium concentration (mg L^{-1}), and R is the removal efficiency (%).

Also the adsorption performance was evaluated by calculating the equilibrium adsorption capacity (qe, mg g^{-1}) using the following Equations (2):

$$qe\ (mg\ g^{-1}) = \frac{(C_0 - C_e)xV}{m}\ x\ 100 \quad (2)$$

where C_0 and C_e are the initial and equilibrium concentrations of pollutants (mg. L^{-1}), V is the volume of the solution (L), and m is the mass of the adsorbent (g).

ANN-Based Modeling Approach

Artificial Neural Networks (ANNs) offer a flexible modeling framework for capturing nonlinear relationships among multiple variables. Due to the nonlinear nature of biosorption processes, a dynamic recurrent network, specifically the Nonlinear Autoregressive with Exogenous Input (NARX), model was chosen.

The NARX architecture incorporates feedback from output nodes to context units, enabling memory of prior states, and enhancing the model's ability to track time-dependent dynamics. This structure leads to improved convergence and generalization compared to traditional feedforward networks.

A total of 175 experimental data points were used to develop the NARX model. These data were randomly partitioned into training (70 %), validation (15 %), and testing (15 %) sets to ensure robust model performance.

The NARX model

The general form of the NARX network is expressed as Equation (3):

$$y(t) = f\,(u\,(t - n_u),\ldots, u(t\text{-}1), u(t), y(t - n_y),\ldots, y(t - 1)) \quad (3)$$

where f is a nonlinear function approximated by the network, u(t) and y(t) are the input and output vectors at time t, n and m are the orders of output and input delays, respectively. In this study, a three-layer NARX network was employed, consisting of: Input layer: 3 neurons (initial concentration, adsorbent dosage, contact time), hidden layer: 10 neurons with tangent sigmoid activation function (tansig), output layer: 1 neuron representing copper removal efficiency. The delay component is denoted by z, and wij, bk, represent the weight and bias parameters of the network, respectively (Coruh et al., 2014).

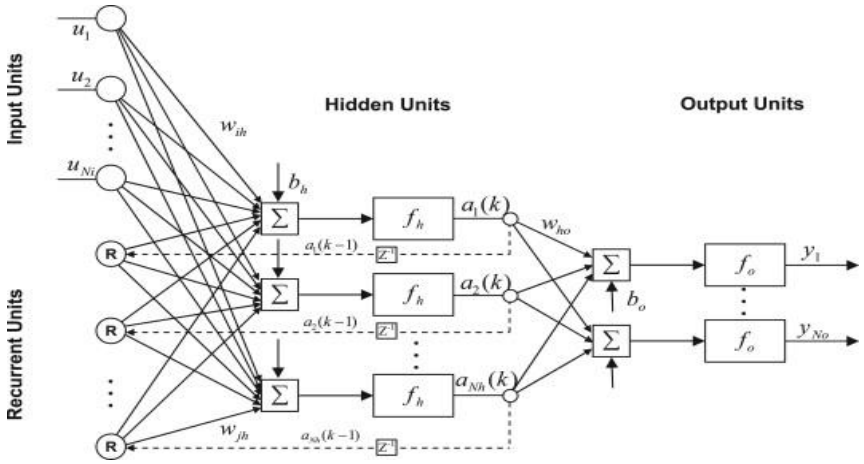

Figure 1. Schematic representation of the NARX neural network used for modeling copper removal efficiency.

During the training phase, the available actual target values are used to compute the error between the predicted and real outputs. These real values are also looped back into the model, enhancing learning stability and making the network operate similarly to a feedforward architecture. When the underlying function f is approximated using a Multilayer Perceptron (MLP), the resulting structure is known as a NARX model. In this study, a three-layer NARX architecture, as illustrated in Figure 1, was employed to estimate the adsorption performance. The network, an input layer including a recurrent unit with 3 neurons (concentration, adsorbent dosage, time), a hidden unit with 10 neurons and an output layer with 1 neuron (removal), is established. In Figure 1, z is the delay element and wij and bk show neural network's weight and bias values, respectively.

Results and Discussion

Biosorbent Preparation and Characterization

The surface morphology of seafood shell biosorbents with varying particle sizes was examined by SEM analysis (Figure 2). The SEM images of seafood shell biosorbents with varying particle sizes (SS and SL) revealed significant differences in surface morphology. The finer particle fraction (SS) displayed a more porous and fragmented surface, whereas the coarser fraction (SL) exhibited a relatively compact and dense morphology with irregular texture. This difference suggests that particle size reduction enhances surface area and exposes more active sites for metal ion interaction, potentially improving biosorption capacity.

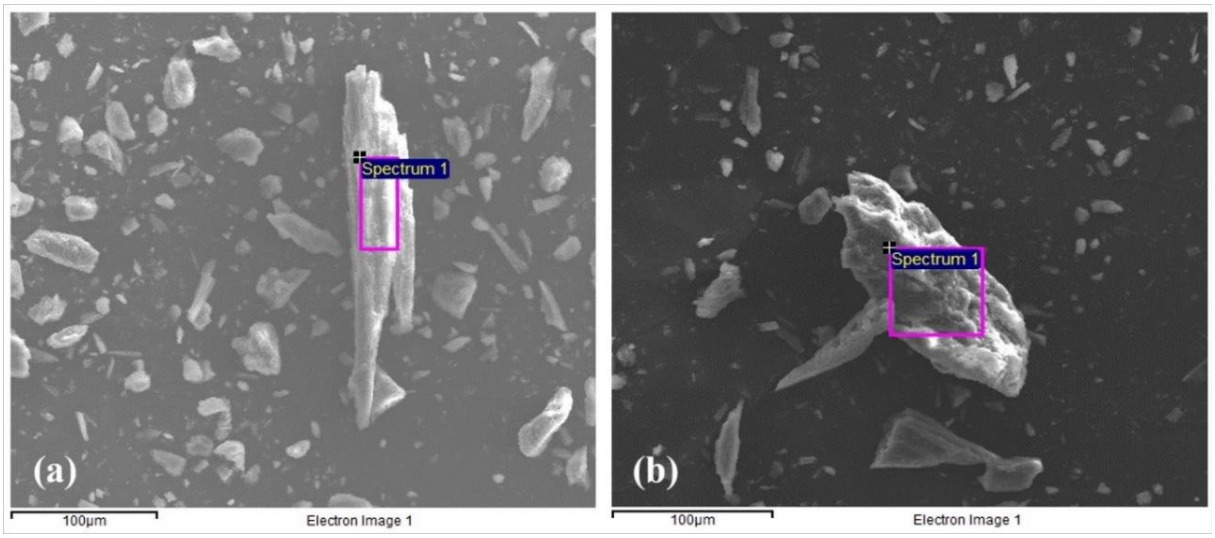

Figure 2. SEM images of seafood shell samples: (a) SS: small particles; (b) SL: large particles

These observations are consistent with previous findings in the literature. For example, Bahadir et al. (2023) reported that reduced particle size in eggshell-derived biosorbents led to increased surface roughness and porosity, resulting in higher Cu^{2+} removal efficiencies. In a similar study, Al-Mur (2024) observed that biosorbents with more open and fragmented surface structures demonstrated superior adsorption behavior due to easier metal ion diffusion.

Moreover, the SS particles' smoother texture may indicate a higher degree of calcium carbonate exposure, which is supported by the enhanced adsorption performance observed in the batch experiments. These findings highlight the critical role of morphological structure in determining biosorption performance, particularly when using naturally occurring materials like seafood shells.

The crystalline structures of the biosorbent samples were analyzed using X-ray diffraction (XRD), as shown in Figure 3.

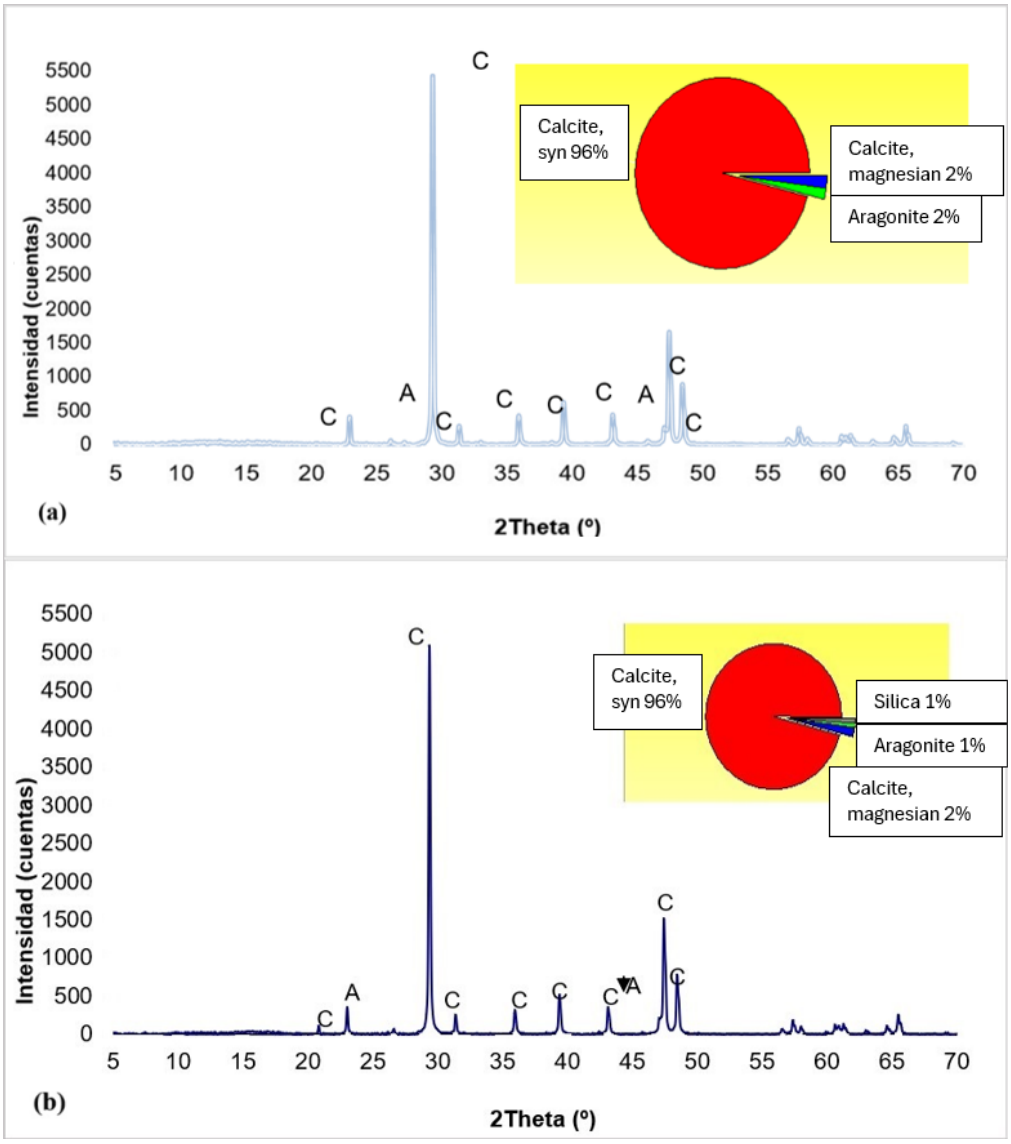

Figure 3. XRD patterns of seafood shell samples: (a) SS: small particle size; (b) SL: large particle size

XRD patterns of both SS and SL samples confirmed that the dominant crystalline phase was calcite ($CaCO_3$), accompanied by minor peaks corresponding to aragonite and silica. The high crystallinity observed suggests that the thermal treatment applied during biosorbent preparation preserved the native calcium carbonate structure without significant transformation. The initial pH of 7.24 is highly favorable for biosorption, as copper ions predominantly exist in the Cu^{2+} form within this range, facilitating effective interaction with the binding sites on the seafood shell surface. Furthermore, the high calcite content of the biosorbent, as confirmed by XRD analysis, likely provided a natural buffering effect that maintained the pH stability throughout the contact time.

This mineral composition aligns with previously reported studies involving marine shell-derived biosorbents. According to the findings of Benazouz et al. (2025) identified calcite as the major phase in mollusk shells used for Pb^{2+} and Cd^{2+} removal, linking the presence of calcite to ion exchange capacity and surface reactivity. Deivayanai et al. (2024) found that calcite-rich biosorbents exhibited high affinity for Cu^{2+} due to the interaction between calcium and heavy metal ions on the surface.

Although both SS and SL samples showed similar mineralogical profiles, the differences in biosorption performance are therefore more likely attributed to physical rather than chemical composition, further emphasizing the importance of particle size and morphology, as revealed in the SEM analysis.

Effect of Particle Size on Copper Removal

As shown in Figure 4, the copper removal efficiency increased with decreasing particle size for both SL and SS biosorbents, reaching a maximum of 91.8 ± 1.2 % at the smallest size range. SS samples consistently outperformed SL counterparts, suggesting that finer particles offer improved adsorption due to larger surface areas and enhanced accessibility to active sites.

Decreasing the particle size led to a simultaneous increase in both removal efficiency and adsorption capacity, with the smallest fraction (-0.063+0.0315 mm) showing the highest qe. This behavior is supported by the SEM results, as smaller particles provide a greater specific surface area and more accessible pores for metal ion capture.

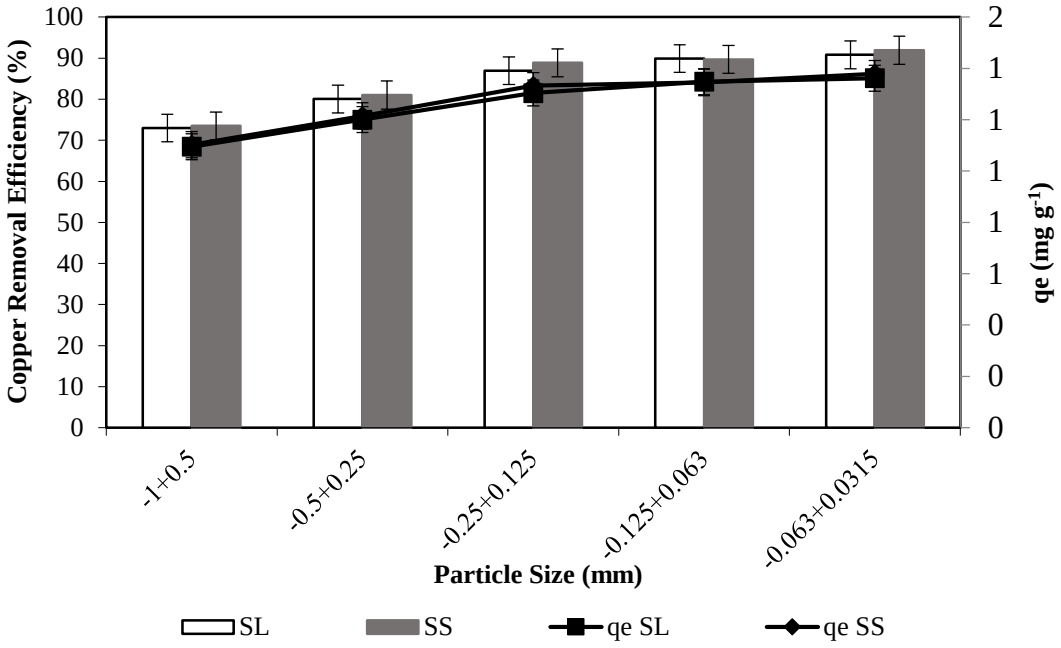

Figure 4. Effect of particle size on copper adsorption efficiency (Conditions: T = 25 °C, Co = 30 mg L^{-1}, dosage = 20 g L^{-1}, contact time = 60min)

SEM analysis provided structural confirmation of this behavior. SS particles exhibited more fragmented and porous surfaces, while SL particles appeared smoother and more compact. This morphology enhances the diffusion of metal ions and interaction with functional groups. Similar conclusions were drawn by findings from Ilaboya and Izinyon (2020), who emphasized the role of porous and irregular biosorbent surfaces in promoting higher adsorption performance. Furthermore, Fiyadh et al. (2023) highlighted that smaller particle sizes increase the external surface area, which contributes to enhanced copper ion capture through physical adsorption mechanisms.

XRD analysis indicated that both SS and SL biosorbents shared a dominant calcite crystalline phase, along with minor aragonite and silica phases, consistent with previous findings reported by Benazouz et al. (2025) on calcium-rich materials. Despite their similar chemical compositions, variations in copper removal efficiency between the two particle fractions are more closely related to their morphological differences rather than mineral content.

Sutherland et al. (2023) also reported that adsorption efficiency is often governed by structural factors such as particle geometry and pore accessibility rather than solely by elemental composition. These findings reaffirm that optimizing particle size and surface structure is critical for enhancing biosorption performance in natural materials such as seafood shells.

Effect of Contact Time on Copper Removal

As illustrated in Figure 5, copper removal efficiency increased rapidly within the first 5 to 15 minutes of contact time for both SS and SL biosorbents, followed by a plateau phase where further increases in time resulted in minimal enhancement of adsorption. This trend suggests that a majority of copper ions were rapidly adsorbed onto available active sites during the initial stage, and equilibrium was nearly achieved by 30-60 minutes.

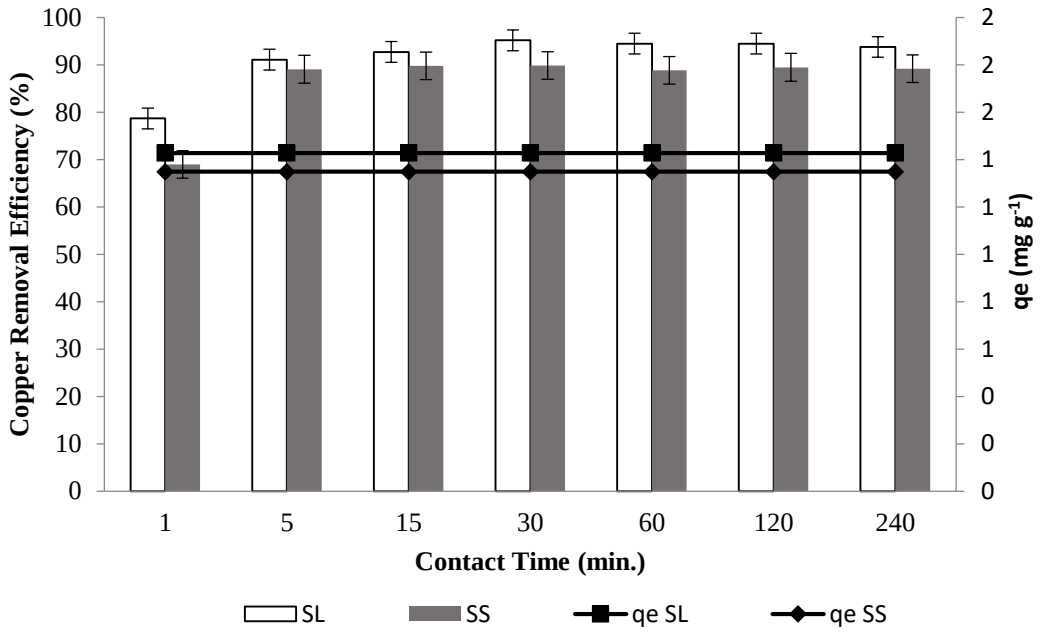

Figure 5. Effect of contact time on copper adsorption efficiency (Conditions: T = 25 °C, Co = 30 mg L^{-1}, dosage = 20 g L^{-1})

The qe values remained relatively stable after 30–60 minutes, confirming that the system reached dynamic equilibrium where the rate of adsorption equals the rate of desorption. The rapid initial increase in qe reflects the abundance of vacant surface sites, which gradually become saturated over time.

Such a pattern is typical of chemisorption or fast surface diffusion processes, as reported in Fiyadh et al. (2023), where biosorbents showed significant metal uptake within the first 10–20 minutes of exposure. The initial sharp rise in removal efficiency is attributed to abundant active binding sites, which gradually become saturated over time.

Furthermore, SS biosorbents consistently exhibited higher adsorption efficiency compared to SL particles across all time intervals. This is likely related to their larger specific surface area and more porous morphology, as previously confirmed by SEM analysis. Similar behavior was described in a study by Bahadir et al. (2023), where smaller particle sizes facilitated faster metal ion diffusion into inner adsorption sites, thereby reducing the equilibrium time.

Although a contact time of 240 minutes was studied, no substantial improvement in copper removal was observed beyond 60 minutes, indicating that the system reached dynamic equilibrium well before the maximum contact time. This observation is in agreement with Samaraweera et al. (2024), who reported that most of the phosphate uptake occurred within the first 60 minutes, after which equilibrium was established due to site saturation (Samaraweera et al., 2024).

Effect of Seafood Shell Dosages on Copper Removal

Figure 6 illustrates the effect of biosorbent dosage (5–40 g L^{-1}) on copper removal efficiency for both SL and SS samples. A marked increase in removal efficiency was observed with increasing biosorbent amounts, particularly between 5 and 20 g L^{-1}. Increasing the dosage from 20 to 40 g L^{-1} provided only a marginal increase in removal efficiency (from ~90% to ~95%), suggesting diminishing returns. Therefore, 20 g L^{-1} (corresponding to 1 g of biosorbent in 50 mL solution) was selected as the optimum dose for further experiments to ensure process economy.

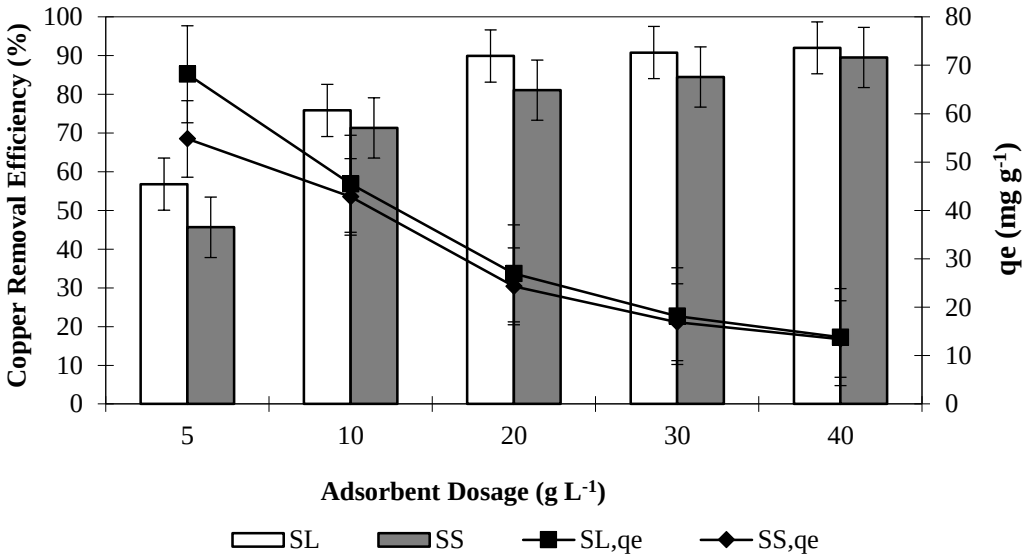

Figure 6. Effect of biosorbent dosage on copper adsorption efficiency (Conditions: T = 25 °C, Co = 30 mg L^{-1}, contact time = 60min)

The adsorption capacity (qe) exhibited an inverse relationship with biosorbent dosage, decreasing from approximately 68 mg g^{-1} to 15 mg g^{-1} as the dose increased from 5 to 40 g L^{-1}. This decline in qe at higher dosages is likely due to the split in the concentration gradient between the solute and the available functional groups, leading to the underutilization of active sites.

The improved performance with increasing dosage can be attributed to a greater surface area and a higher number of active functional groups, as suggested by SEM observations which revealed more accessible surface textures in SS samples. The slightly higher performance of SS particles across all dosages further confirms that smaller particles with fragmented surfaces provide more effective metal interaction sites.

Similar trends were reported by Ilaboya and Izinyon (2020), where increasing the dose from 1.0 to 5.0 g L^{-1} led to improved removal, and Al-Mur (2024), who utilized dosages up to 10.0 g L^{-1} for mollusk shells. While our study employed higher dosages (5–40 g L^{-1}) to account for the raw (unmodified) nature of the seafood shells, the overall mechanism of enhanced site availability remains consistent with these findings.

However, the increment in efficiency began to plateau beyond 30 g L^{-1}, likely due to the aggregation of particles and overlapping of adsorption sites, which reduces the effective surface area a phenomenon also according to Sutherland et al. (2023). This suggests that while increasing dosage is beneficial up to a certain point, excess biosorbent may lead to diminishing returns in removal efficiency. Therefore, beyond the optimum dosage of 20 g L^{-1}, the rate of increase in removal efficiency slows down significantly due to the overlapping of active sites.

Effect of Initial Copper Concentration

As shown in Figure 7, copper removal efficiency increased significantly with rising initial Cu^{2+} concentrations from 10 to 30 mg L^{-1} for both SL and SS biosorbents, reaching a plateau beyond this point. The highest removal efficiency (~95 %) was achieved at 40 and 50 mg L^{-1} (yielding 94.6±1.1 % and 95.1±0.9 %, respectively), indicating saturation of active sites and a near-equilibrium state.

This trend can be attributed to the enhanced mass transfer driving force at higher metal concentrations, which improves the diffusion rate of Cu^{2+} ions toward the biosorbent surface. Similar findings were reported by Deivayanai et al. (2024), who observed increased Cu^{2+} uptake by calcite-rich biosorbents with higher initial ion concentrations due to stronger concentration gradients.

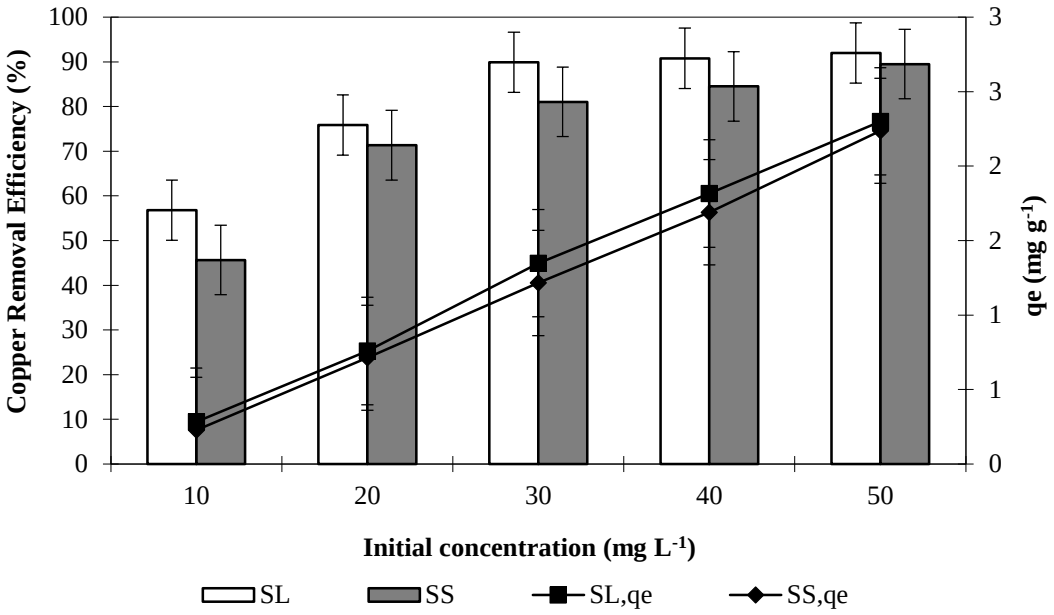

Figure 7. Effect of initial copper concentration on adsorption (Conditions: T = 25 °C, dosage = 20 g L^{-1}, contact time = 60min)

SS biosorbents consistently outperformed SL counterparts at each concentration level, further confirming the influence of particle size and surface area. This is consistent with the journal article in (Benazouz et al. 2025), where finer biosorbents provided better accessibility to binding sites, particularly under conditions of higher metal ion loading.

While the removal efficiency reached a plateau, the adsorption capacity (qe) increased significantly from approximately 0.5 to 2.5 mg g^{-1} as the initial concentration rose to 50 mg g^{-1}. This trend is attributed to the enhanced concentration gradient, which acts as a powerful driving force to overcome the mass transfer resistance between the aqueous and solid phases.

However, beyond 30 mg L^{-1}, the increase in removal efficiency diminished, likely due to saturation of available adsorption sites, a phenomenon also noted in the study by Alshahrani et al. (2024), where biosorption equilibrium was approached at elevated concentrations. These results suggest that while increasing initial concentration promotes adsorption to a point, biosorbent dose and surface saturation ultimately govern performance limits.

Adsorption Isotherms Models

The isotherm model parameters presented in Table 1 indicate that the Freundlich model best described the copper biosorption process for both SL and SS samples, as evidenced by the highest correlation coefficients (R^2 = 0.89 for SL and 0.93 for SS). This suggests that the adsorption process occurs on a heterogeneous surface and involves multilayer adsorption, which is typical for biosorbents derived from natural materials.

The Freundlich constant n was greater than 1 for the SS sample (1.08), indicating favorable adsorption. The higher KF value for SS (3.58 mg g L^{-1}) compared to SL (3.06 mg g L^{-1}) further supports the greater affinity of the smaller particle-sized biosorbent for copper ions. This behavior is consistent with the surface morphology observations made via SEM, which revealed more fragmented and porous surfaces in SS samples, promoting multilayer interaction with metal ions.

Table 1. Isotherm model parameters for copper biosorption onto seafood shells

Isotherm	Linear Equation	Parameter	SL	SS
Langmuir	$\frac{Ce}{qe} = \frac{1}{q_{max}.K_L} + \frac{1}{q_{max}}Ce$	q_{max} (mg g^{-1})	11.54	95.23
		B (L mg^{-1})	0.028	24.52
		R^2	0.06	0.001
Freundlich	$Log(qe) = Log(K_F) + \frac{1}{n}Log(Ce)$	n	0.88	1.08
		K_F (mg g L^{-1})	3.06	3.58
		R^2	0.89	0.93
Temkin	$qe = B.Ln(Ce) + B.LnK_T$	K_t (L g^{-1})	1.200	0.924
		α_t (J mol^{-1})	1.01	1.08
		R^2	0.85	0.79

Conversely, the Langmuir model provided a poor fit to the experimental data, as reflected by very low R^2 values (0.06 for SL and 0.001 for SS). This implies that monolayer adsorption on homogeneous surfaces is not the dominant mechanism in this system. Although the mathematical resolution of the Langmuir equation yielded a high theoretical maximum adsorption capacity (qmax) of 95.23 mg g^{-1} for the SS biosorbent, the low correlation coefficient indicates that this specific value should be interpreted with caution. Consequently, the adsorption behavior is more accurately defined by the heterogeneous surface interactions described by the Freundlich model rather than a monolayer limit.

The Temkin model provided moderate correlation (R^2 = 0.850 for SL, 0.790 for SS), implying that interactions between adsorbate and adsorbent play a non-negligible role. The Temkin constants (B and α_t) suggest that heat of adsorption remains within a moderate range, indicating the predominance of chemisorption, particularly for the SS sample.

These observations align well with literature findings. This is consistent with the results presented by Deivayanai et al. (2024) and Alshahrani et al. (2024) both reported that biosorbents derived from calcium carbonate-rich materials displayed nonlinear and heterogeneous adsorption behavior best captured by the Freundlich model. They emphasized that such biosorbents exhibit variable energy sites that favor multilayer adsorption, especially when surface area is enhanced through particle size reduction.

Adsorption Kinetics Models

The kinetic data for copper biosorption onto both SS and SL seafood shell biosorbents were best described by the pseudo-second-order (PSO) model, as indicated by the extremely high correlation coefficients ($R^2 = 0.99$ for both), as shown in Table 2.

This suggests that the biosorption process is predominantly governed by chemisorption involving valency forces through the sharing or exchange of electrons between copper ions and functional groups on the biosorbent surface.

In contrast, the pseudo-first-order model provided a poor fit, with R^2 values of 0.29 and 0.05 for SS and SL, respectively. The intraparticle diffusion model showed moderate correlation ($R^2 = 0.32$ for SS and 0.23 for SL), suggesting that while diffusion into internal pores contributed to the overall rate-limiting step, it was not the sole controlling mechanism.

Table 2. Kinetics model parameters for copper biosorption onto seafood shells

Kinetic	**Linear Equation**	**Parameter**	**SS**	**SL**
Pseudo-First-Order	$Ln(qe - qt) = k_1.t + Ln(qe)$	k_1(L min^{-1})	0.0071	0.0041
		qe (mg g^{-1})	17.98	50.86
		R^2	0.29	0.05
Pseudo-Second-Order	$\frac{t}{qt} = \frac{1}{qe}.t + \frac{1}{k_2.qe^2}$	q_e (mg g^{-1})	1.4	1.33
		k_2 (g mg min^{-1})	7.62	53.33
		R^2	0.99	0.99
Intraparticle Diffusion	$qt = k_i.t^{1/2} + C$	k_i (g mg min^{-1})	0.0097	0.0108
		C	1.3	1.22
		R^2	0.32	0.23

These results align well with previous studies. For instance, research by Al-Mur (2024) and Ilaboya and Izinyon (2020) reported similar findings for calcium-rich and porous biosorbents, where the PSO model demonstrated superior agreement with experimental data, reflecting the involvement of surface complexation and ion exchange mechanisms. Overall, the superior kinetic fit of the PSO model across both biosorbents reinforces that chemisorption dominates the removal mechanism, regardless of particle size.

Data Analysis

To determine the statistical significance of the operational parameters, a one-way analysis of variance (ANOVA) was performed. The results indicated that the effect of particle size reduction on copper removal was statistically significant with a p-value less than 0.05 ($p < 0.05$).

Modeling With NARX Neural Network

The modeling results obtained using the NARX (Nonlinear Autoregressive with Exogenous Inputs) neural network architecture demonstrate strong predictive capacity for copper removal efficiency. As shown in Figure 8, the mean

squared error (MSE) values for training, validation, and testing datasets converged smoothly, reaching a minimum validation error of 3.8127×10^{-5} at epoch 14. This low error level indicates the robustness of the model in learning from experimental data without significant overfitting or underfitting.

Table 3. NARX neural network training parameters

Parameter	**Value**
Number of input nodes	3
Number of output nodes	1
Hidden layer neurons	10
Activation function	Tangent sigmoid (tansig)
Training algorithm	BP-GDM
Epochs	100
Error goal (MSE)	0.001
Learning rate (μ)	0.00001

The training parameters provided in Table 3, including 3 input nodes, 1 output node, 10 hidden layer neurons, and a tangent sigmoid activation function, are consistent with configurations reported by Bashir et al. (2020), Biswas et al. (2024), Fiyadh et al. (2023) that successfully modeled heavy metal biosorption using ANN architectures. The selection of backpropagation with gradient descent momentum (BP-GDM) and a small learning rate (μ=0.00001) further contributed to the model's stability during optimization.

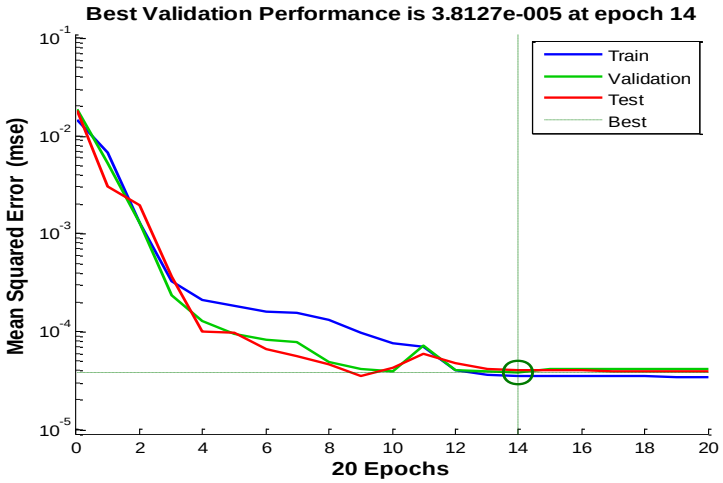

Figure 8. Training performance of the NARX neural network (MSE vs. epochs)

The input and output data ranges used for training, validation, and testing the NARX neural network are summarized in Table 4. These ranges were carefully selected to ensure the model's capacity to learn underlying patterns and to generalize effectively across different experimental conditions.

The training and validation datasets covered moderate ranges of concentration (10–40 mg L^{-1}), contact time (1–180 min), and adsorbent dosage (5–30 g L^{-1}), enabling the model to develop a stable learning foundation while avoiding overfitting to extreme values. These ranges also encompassed a wide removal efficiency spectrum (45–90%), which allowed the network to capture nonlinear interactions among variables.

Table 4. Input and output data ranges used for NARX model

Parameter	**Training Data**	**Validation Data**	**Testing Data**
Concentration (mg L^{-1})	10 – 40	10 – 40	10 – 50
Time (min)	1 – 180	1 – 180	1 – 240
Adsorbent dosage (g L^{-1})	5 – 30	5 – 30	5 – 40
Removal efficiency (%)	45 – 90	45 – 90	45 – 93

The testing dataset included the extreme values of the experimental design namely, 50 mg L^{-1} initial concentration, 240 minutes contact time, and 40 g L^{-1} adsorbent dosage making it suitable for evaluating the model's extrapolation capability. This approach allowed for an assessment of the model's robustness when applied to data outside the central range of training, which is particularly valuable for predictive modeling in real-world applications.

Overall, the well-distributed and representative segmentation of the data ensured that the NARX model could generalize effectively, as evidenced by its high predictive accuracy and low mean squared error (MSE) observed during performance evaluation. This data partition strategy is consistent with the approaches reported by Fiyadh et al. (2023) and Ilaboya and Izinyon, (2020) where similar ANN-based modeling frameworks were successfully applied to environmental systems.

Conclusions

This study demonstrated the effectiveness of waste seafood shells as a low-cost and eco-friendly biosorbent for the removal of copper ions from aqueous solutions. The experimental results revealed that adsorption performance was strongly influenced by particle size, contact time, adsorbent dosage, and initial Cu^{2+} concentration. Smaller particle sizes exhibited enhanced removal efficiency due to increased surface area and pore availability.

The experiments were conducted at a constant initial pH of 7.24, which represents a limitation of the current study. Since pH is a critical factor in heavy metal adsorption, future research should explore a wider pH range to determine the point of zero charge (pH_{pzc}) of the seafood shells and its impact on copper speciation.

Isotherm modeling indicated that the adsorption process followed the Freundlich model more closely than the Langmuir or Temkin models, suggesting a multilayer adsorption mechanism on a heterogeneous surface. Kinetic data were best described by the PSO model, implying that chemisorption played a dominant role in copper uptake.

Morphological and structural characterization of the biosorbents through SEM and XRD analyses provided valuable insights into the relationship between surface features and adsorption performance. SEM images confirmed that the finer shell fraction had a rougher and more porous surface texture, while XRD patterns verified the predominance of calcite as the major crystalline phase, supported by minor contributions of aragonite and silica.

Furthermore, a NARX artificial neural network model was successfully developed to predict Cu^{2+} removal efficiency based on operational parameters. The model achieved high predictive accuracy, with consistent performance across training, validation, and testing datasets. This approach not only enhanced the understanding

of process dynamics but also provided a reliable computational tool for simulating and optimizing biosorption systems.

Although the ANN model did not directly perform optimization, it helped us better understand the biosorption process and created a solid basis for identifying more efficient operating conditions in future work.

Overall, this research highlights the promising potential of seafood shell waste in sustainable wastewater treatment and demonstrates the synergistic power of combining experimental methods with machine learning techniques for environmental applications.

From an industrial perspective, the abundance and zero-cost nature of seafood shells make them attractive for large-scale wastewater treatment. Future studies should investigate the regeneration potential of these shells using mild acidic desorbing agents to evaluate their reusability over multiple cycles, which would further enhance the process's circular economy footprint.

Conflict of Interest

The author(s) declare that there is no conflict of interest regarding the publication of this manuscript.

References

Al-Mur, B. 2024. Application of marine mollusk shells (meretrix lusoria) as low-cost biosorbent for removing cd2+ and pb2+ ıons from aqueous solution: kinetic and equilibrium study. *Water*, 16(18): 2615.

Alshahrani, T., Jethave, G., Nemade, A., Khairnar, Y., Fegade, U., Khachane, M., Ahmed, A., and Khan, F. (2024). Application of ann, hypothesis testing and statistics to the adsorptive removal of toxic dye by nanocomposite. *Chemometrics and Intelligent Laboratory Systems*, 249: 105132.

Bahadir, T., Gülden, G., Çelebi, H., Şimşek, İ., and Gök, O. 2023. Seafood wastes as an attractive biosorbent: Chitin-based shrimp shells. *Water, Air, & Soil Pollution*, 234(3): 145.

Bashir, M., Tyagi, S., and Annachhatre, A.P. 2020. Adsorption of copper from aqueous solution onto agricultural adsorbents: kinetics and isotherm studies. *Materials today: Proceedings*, 28: 1833-1840.

Benazouz, K., Bouchelkia, N., Moussa, H., Boutheldja, R., Zamouche, M., Amrane, A., Parvathiraja, C., Al-Lohedan, H., Bollinger, J., and Mouni, L. 2025. Efficient removal of cu (II) from wastewater using chitosan derived from shrimp shells: a kinetic, thermodynamic, optimization, and modelling study. *Water*, 17(6): 851.

Biswas, S., Lodh, B.K., Das, J., Nag, S., and Mishra, U. 2024. Experimental study and ANN verification of chemically carbonized hevea brasiliensis sawdust for adsorption of hexavalent chromium. *Biomass Conversion and Biorefinery* 15(6): 9271-9281.

Coruh, S., Geyikci, F., Kilic, E., and Coruh, U. 2014. The use of NARX neural network for modeling of adsorption of zinc ions using activated almond shell as a potential biosorbent. *Bioresour Technology*, 151: 406-410.

Deivayanai, V.C., Karishma, S., Thamarai, P., Saravanan, A., and Yaashikaa, P.R. 2024. Efficient red azo dye removal from wastewater using magnetic nanoparticle impregnated prosopis juliflora biomass: ANN modeling approach. *Desalination and Water Treatment*, 320: 100746.

Dharmendra, T.A. 2024. Electrocoagulation process modelling and optimization using RSM and ANN-GA for simultaneous removal of arsenic and fluoride. *Multiscale and Multidisciplinary Modeling, Experiments and Design*, 7(6): 5899-5914.

Dutta, S.K., Jahan, M.N., Kaur, N., Barna, S.D., Sathi, N.J., Sultana, R., and Amin, M.K. 2024. Banana leaves powder as an effective, low-cost adsorbent for methyl blue dye removal: kinetics, isothermal, thermodynamics, ANN and DFT analysis. *International Journal of Environmental Science and Technology*, 22(3): 1865-1890.

El Haddad, M., Regti, A., Laamari, M.R., Slimani, R., Mamouni, R., Antri, S., and Lazar, S. 2014. Calcined mussel shells as a new and eco-friendly biosorbent to remove textile dyes from aqueous solutions. *Journal of the Taiwan Institute of Chemical Engineers*, 45(2): 533-540.

Fiyadh, S.S., Alardhi, S.M., Al Omar, M., Aljumaily, M.M., Al Saadi, M.A., Fayaed, S.S., and El-Shafi, A. 2023. A comprehensive review on modelling the adsorption process for heavy metal removal from waste water using artificial neural network technique. *Heliyon*, 9(4): e15455.

Ilaboya, I.R., and Izinyon, O.C. 2020. Modelling, optimization and prediction of sorption of Pb(II) and Mn(II) ions from wastewater onto acid activated shale using adaptive neuro fuzzy inference systems (ANFIS), response surface methodology (RSM) and modular neural network (MNN). *International Journal of Engineering Science and Application*, 4(1): 1-22.

Kusmierek, K., Swiatkowski, A., Zienkiewicz-Strzalka, M., and Marczewska, A. 2025. Studies of the kinetics and isotherms of copper ions adsorption on APTES-modified silica materials. *Desalination and Water Treatment*, 321: 100965.

Monteiro, R.J.R., Lopes, C.B., Rocha, L., Coelho, J.P., Duarte, A.C., and Pereira, E. 2016. Sustainable approach for recycling seafood wastes for the removal of priority hazardous substances (Hg and Cd) from water. *Journal of Environmental Chemical Engineering*, 4(1): 1199-1208.

Samaraweera, H., Zahir, A., Alam, S.S., Perera, S.S., Masud, M.A.A, Khan, A.H., Oguntuyi DO, Yunusu W, Shin WS, Mohamed, M.M., and Mlsna, T. 2024. Sustainable utilization of Fe_3O_4-modified activated lignite for aqueous phosphate removal and ANN modeling. *Environmental Research*, 260: 119618.

Sutherland, C., Chittoo, B.S., and Samlal, A. 2023. The status of scientific development on the application of biosorption of heavy metals at laboratory and pilot-scale: A review. *Desalination and Water Treatment*, 299: 13-49.